https://doi.org/10.5194/egusphere-2025-5492
Preprint. Discussion started: 15 December 2025

Sub-seasonal variability and multi-year trends in glacier area change and ice speed on the Antarctic Peninsula

Sarah Leibrock[1,2], Ross A. W. Slater[3], Anna E. Hogg[3] and Celia A. Baumhoer[1]

[1]Land Surface Dynamics Department, German Remote Sensing Data Center (DFD), German Aerospace Center (DLR), Wessling, D-82234, Germany
[2]Institute for Geography and Geology, University of Würzburg, D-97074 Wuerzburg, Germany
[3]School of Earth and Environment, University of Leeds, Leeds, West Yorkshire, LS2 9JT, United Kingdom

Correspondence to: Sarah Leibrock (sarah.leibrock@uni-wuerzburg.de)

Abstract. As the climate continuous to warm, glaciers on the Antarctic Peninsula (AP) are experiencing rapid dynamic changes, including accelerated rates of thinning, terminus retreat, and ice flow, all of which have significant implications for global sea level rise and climate feedback mechanisms. These glaciological changes unfold over varying timescales spanning from months to decades, necessitating temporally and spatially detailed monitoring. Here, we used sub-seasonal records of terminus area change (2013–2023) together with high-resolution satellite-derived ice surface velocity measurements (2014–2024) to investigate the evolution of 42 key outlet glaciers on the northern AP. We found that during the past decade, these glaciers underwent substantial but spatially heterogeneous changes in terminus position and ice flow velocity. Cumulative ice loss amounted to ~279 km², with 73 % of this loss occurring on the eastern side, particularly within the Larsen B embayment. By contrast, western glaciers showed smaller, more variable responses. Overall, 71 % of glaciers accelerated, though most eastern glaciers displayed slight trends of slowdown – except in the Larsen B region, where major calving events beginning in early 2022 were followed by drastic increases in velocity, with some glaciers more than doubling their flow speed. In addition, a seasonality analysis revealed widespread inter-annual variability: two-thirds of glaciers showed strong to very strong seasonal fluctuations in flow speed, and about half exhibited comparable signals in terminus change. Cross-correlation analysis further indicated that, for most glaciers, terminus area changes and ice velocity dynamics had only minimal influence on one another. These results highlight the spatially and temporally heterogeneous nature of glacier dynamics on the northern AP, suggesting that glacier change in this region is shaped by a combination of environmental drivers and glacier-specific factors operating on widely varying timescales. They underscore the need for detailed, high-resolution observations and continuous monitoring to improve the understanding of glacier evolution under ongoing climatic and environmental change.

1 Introduction

The Antarctic Peninsula (AP) is among the most rapidly warming regions on Earth, with air temperatures rising by approximately 3°C between 1951 and 2019 (Carrasco et al., 2021). At the same time, ocean temperatures at the seabed along the western AP and in the Bellingshausen Sea have increased by 0.1–0.3°C per decade since the 1990s (Schmidtko et al., 2014). This combined atmospheric and oceanic warming has been associated with a series of substantial glaciological changes,

https://doi.org/10.5194/egusphere-2025-5492
Preprint. Discussion started: 15 December 2025

including the retreat and collapse of several large ice shelves, such as the Wordie Ice Shelf (1996 to 1989), Prince Gustav Ice Shelf (1989 to 1995), Larsen A Ice Shelf in 1995, and Larsen B Ice Shelf in 2002 (Rott et al., 2002; Rott et al., 1996; Cook and Vaughan, 2010; Doake and Vaughan, 1991; Rack et al., 1998; Scambos et al., 2003). After the collapse of Larsen B in 2002, multi-year landfast sea ice formed in the embayment in 2011 and persisted until January 2022, when it fractured and broke up within a few days (Ochwat et al., 2024). Following this collapse – and after a decade of gradual deceleration and advance – tributary glaciers underwent dramatic retreat of up to 23 km within 1.5 years (Fluegel and Walker, 2024; Ochwat et al., 2024) and accelerated by 20 %–50 % by the end of 2022 (Surawy-Stepney et al., 2024). Alongside these events, many glaciers across the AP have experienced retreat and acceleration in recent decades (Davison et al., 2024). For the northern AP, Seehaus et al. (2018) reported a total loss of glacier area of 238.81 km² between 1985 and 2015, while Kang et al. (2024) observed a general acceleration in ice flow after 2020. However, these glaciological changes did not occur uniformly across the peninsula. The largest ice losses were recorded for glaciers affected by ice shelf disintegration, where the subsequent loss of buttressing significantly weakened the stability of tributary glaciers, leading to dramatic increases in ice discharge, accelerated flow, and frontal retreat (Rack and Rott, 2004; Rignot et al., 2004; Seehaus et al., 2015; Wendt et al., 2010). Significant changes have also been observed for tidewater glaciers that do not terminate into ice shelves, such as most glaciers along the western coast of the AP. These glaciers have experienced retreat, acceleration, and thinning since at least the 1980s, with flow speeds increasing by an average of 41 % between 1992 and 2014 (Cook et al., 2005; Cook and Vaughan, 2010; Cook et al., 2014; Seehaus et al., 2018). More recently, ice discharge from western glaciers has more than tripled, rising from 50 Mt yr^{-1} during 2017–2020 to 160 Mt yr^{-1} in 2023, likely in response to ocean warming (Davison et al., 2024). Beyond these long-term trends, Wallis et al. (2023b) showed that glaciers along the western AP exhibited pronounced seasonal variability, with summer speed-ups averaging 12.4 ± 4.2 %, linked to changes in terminus position, surface melt, precipitation inputs, and ocean temperature. Collectively, these patterns indicate that glaciers on the AP are sensitive indicators of climate change, exhibiting significant spatial variability and responding on different timescales to shifts in environmental conditions. Consequently, to effectively monitor and understand glacier changes in this region, it is crucial to obtain both spatially and temporally detailed observations, as emphasized by Seehaus et al. (2018).

In this context, Earth observation (EO) datasets that capture glaciological variables such as ice velocity or calving front dynamics at intra-annual timescales remain scarce. This limitation arises because monitoring short-term and sub-seasonal glacier dynamics on the AP is particularly challenging. Factors such as the small size and fast ice flow of its glaciers, along with the region's complex topography, variable climate, and extreme weather conditions, complicate the extraction of ice dynamic variables from remote sensing data. For example, high snowfall and surface melt can alter radar backscatter, hindering the tracking of glacier displacement and derivation of ice velocity measurements (Wallis et al., 2023a; Rott et al., 2021). Similarly, calving front positions are often delineated manually, a time-consuming process that limits both spatial and temporal coverage despite the growing availability of satellite imagery (Loebel et al., 2025; Baumhoer et al., 2018).

In this study, we leverage a newly developed, temporally and spatially dense glacier terminus area dataset from Loebel et al. (2025) and combine it with high resolution ice surface velocity measurements to investigate the recent dynamics of 42 outlet

https://doi.org/10.5194/egusphere-2025-5492
Preprint. Discussion started: 15 December 2025

glaciers across the AP from 2013–2024. By integrating these complementary datasets, our analysis captures glacier changes at a seasonal to sub-seasonal resolution, providing new insights into short-term variability as well as interannual trends in glacier flow and terminus area changes.

2 Study area

This study focuses on the northern part of the AP, known as Graham Land (Fig. 1). The area stretches from the George VI Ice Shelf in the South (70° S) to Trinity Peninsula in the North (63° S) and is bordered by the Bellingshausen Sea to the West and the Weddell Sea to the East (Carrasco et al., 2021; Seehaus et al., 2018; Stewart, 2011). The landscape is characterized by an intricate mountainous terrain, gradually rising from the coastal regions to flat, snow covered plateaus above 1,500 m (Carrasco et al., 2021; Dong et al., 2021). This mountain chain acts as a natural orographic divide, creating pronounced west-to-east gradients in atmospheric and ocean circulation, as well as distinct differences in glaciological characteristics on either side of the peninsula (Carrasco et al., 2021; Silva et al., 2020; Siegert et al., 2019; Huber et al., 2017). Climatologically, the western side is defined by a sub-polar climate with mean annual air temperatures ranging from −1 °C to −7 °C. The eastern side in contrast, is characterized by a polar continental climate, with air temperatures between −7 °C and −14 °C (Carrasco and Cordero, 2020; Carrasco et al., 2021). Since the early 1950s, both air and ocean temperatures across the entire AP have shown a general warming trend. However, a cooling period prevailed from the late 1990s until mid-2010s, after which air temperatures began rising again, with an increase of approximately +0.36°C by 2020 (Huber et al., 2017; Carrasco et al. 2021). This long-term trend of atmospheric warming has been associated with ice shelf recession and disintegration beginning in the 1980s (Scambos et al., 2003) and with surface melt induced glacier acceleration, particularly in recent decades (Wallis et al., 2023b; Tuckett et al., 2019). At the same time, the rising ocean heat content in the Bellingshausen Sea has been shown to strongly affect glacier dynamics along the western AP, promoting acceleration, retreat, and dynamic thinning (Cook et al., 2016; Wallis et al., 2023a; Seehaus et al., 2018).

This study focuses on 42 marine-terminating glaciers (Fig. 1), with catchments extending from the high elevation interior plateaus down to the ocean. Of these glaciers, 30 are situated on the western side, while the remaining 12 are located on the eastern side within the embayments of previously collapsed ice shelves (Prince Gustav Ice Shelf, Larsen Inlet, Larsen A, and Larsen B).

https://doi.org/10.5194/egusphere-2025-5492
Preprint. Discussion started: 15 December 2025

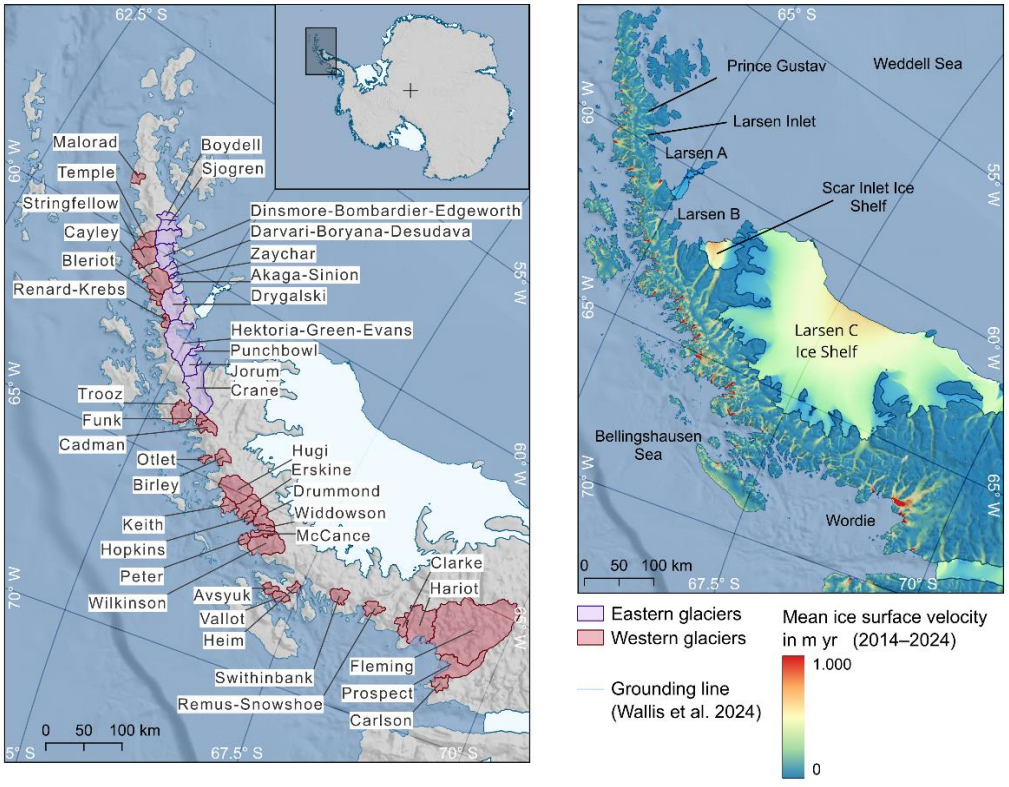

Figure 1. (a) Map of the study area showing the catchments (derived from Antarctic Digital Database (ADD) 7.10 (Cook et al., 2014)) and names of the investigated 42 glaciers on the AP. Glaciers are coloured based on their geographical location on the eastern (purple) or western (dark red) coast. (b) Map showing the mean ice speed (km yr^{-1}) on the AP (December 2014–February 2024) (Slater et al., In Prep), providing geographic and oceanographic context of the study region. Background: ADD coastline v7.10. (Gerrish et al., 2024), Bedmap3 (Pritchard et al., 2024).

3 Data and methods

In order to derive temporally and spatially dense information on changes in glacier dynamics, we analysed various remote sensing datasets. Glacier terminus area changes were obtained from the recently published dataset of Loebel et al. (2025). Surface velocity fields were computed from repeat-pass synthetic aperture radar (SAR) satellite acquisitions and were used to quantify changes in glacier flow speed. Additionally, we used auxiliary vector data from Wallis et al. (2024) to identify the location of the grounding line using the differential range direction offset tracking (DROT) technique, and glacier inventory data from the Antarctic Digital Database (ADD) 7.10 (Cook et al., 2014) to delineate glacier basins for visualization. Glacier names were adopted from the terminus area dataset of Loebel et al. (2025) and compound names were abbreviated (Darvari-Boryana-Desudava – DBD, Dinsmore-Bombardier-Edgeworth – DBE, Hektoria-Green-Evans - HGE).

https://doi.org/10.5194/egusphere-2025-5492
Preprint. Discussion started: 15 December 2025

3.1 Terminus area changes

The dataset of Loebel et al. (2025) provides calving front positions and terminus area changes at sub-seasonal resolution for 42 tidewater glaciers in the study area from 2013–2023. As the data were derived from optical imagery, the time series contain a 14-week gap during polar night from May to mid-August. Outside this period, the dataset provides an average resolution of 19.5 days, although the sampling is irregular and primarily dependent on satellite orbit and cloud cover. The exact temporal coverage for each glacier can be found in Loebel et al. (2025). The dataset was created using a deep learning based processing system developed to automatically delineate glacier calving fronts from multispectral Landsat-8 and Landsat-9 imagery. The final data product includes 4,817 calving front positions, which were then used to calculate terminus area changes using the rectilinear box method. Terminus area changes are provided as relative values, referenced to the first measurement of the respective time series.

For the analysis of glacier terminus area changes, the time series were resampled to monthly median values to mitigate irregular sampling intervals and improve temporal consistency. The linear trend for each time series was then calculated using linear regression with the scipy.stats.linregress function (Virtanen et al., 2020). Additionally, the PiecewiseLinFit function from the pwlf library (Jekel and Venter, 2019) was employed to perform piecewise linear fitting, which allowed for the detection and modelling of shifts in the data. This was used for validating visually identified change points in certain time series. After visually inspecting the plotted time series and their respective trends, we manually grouped them into four categories based on the evolution of terminus area changes, the statistical significance of the trends, and the presence of pronounced change points (see Table 1).

Table 1. Description of the terminus area and velocity change categories.

Category	Description
Acceleration/ advance	Significant ($p < .05$) positive trend of ice flow speed (acceleration)/ terminus area changes (advance)
Deceleration/ retreat	Significant ($p < .05$) negative trend of ice flow speed (deceleration)/ terminus area changes (retreat)
Fluctuating	Non-significant ($p > .05$) linear trends of ice flow speed/ terminus area changes, short-term fluctuations
Change Point	Reversal in trend during the study period. Negative to positive for ice flow speeds and positive to negative for terminus area changes

3.2 Ice surface velocity

The ice velocity measurements used in this study are derived from Sentinel-1 (S1) SAR data acquired between October 2014 and February 2024 (Davison et al., 2025). Our methods follow Davison et al. (2025) and Slater et al. (In Prep.), both of which build on earlier S1 ice velocity processing methodology (Hogg et al., 2017; Lemos et al., 2018). Ice surface displacements were calculated from offset tracking (Strozzi et al., 2002) of sequential S1 image pairs using the GAMMA remote sensing software (Werner et al., 2000). Offset tracking was performed using Single Look Complex (SLC) images acquired in

https://doi.org/10.5194/egusphere-2025-5492
Preprint. Discussion started: 15 December 2025

Interferometric Wide Swath (IW) mode, with horizontal-transmit / horizontal-receive (HH) polarization (the standard acquisition mode over the Antarctic Ice Sheet). Image pairs were separated by either 6 or 12 days depending on the availability of imagery from the Sentinel-1A and Sentinel-1B satellites, due to variations on their acquisition plans and operational period. In offset tracking, small sections of these images (windows) are compared at regular intervals (steps), at each of which cross-correlation is performed, and the location of the peak of the correlation function is also used to generate a spatially varying estimate of error (Lemos et al., 2018). We average across five combinations of these step and window sizes (Tab. 2) to ensure optimum coverage across the complex terrain of the AP.

All observations with matching start and end image dates were then mosaiced onto a standard polar stereographic grid at 100 m posting and filtered to remove outliers from individual velocity fields (Davison et al., 2025). Filtered mosaics were then converted from a stack of GeoTIFF files to chunked Zarr stores in which each chunk has a small spatial footprint (250 x 250 pixels) but is continuous in time. This allows for rapid extraction of time series from our dataset and computational efficiency when processing large volumes of time series data (Slater et al. (In Prep.)). We then resampled time series to daily averages to account for different image pairs having same mid-date (used to order the observations) due to varying lengths of image pair separation.

Temporal outlier removal was performed using a two-step filter. First, we generated an outlier-robust estimate of the standard deviation using the median absolute deviation (MAD). We approximated $\hat{\sigma}_{ts}$, the outlier-robust standard deviation for the entire time series, by multiplying the MAD by a constant $\kappa = 1.4826$ and then used rolling thresholds at two different time scales to remove outliers at coarse and then fine temporal resolution. Data points with an absolute difference $>5\hat{\sigma}_{ts}$ from a 1-year rolling median were first removed, before a Hampel filter with a rolling window size of 90-days is applied. Data points with an absolute difference $> 2\hat{\sigma}_{window}$ from the 90-day window median were removed as a result. Finally, time series were smoothed using a Bayesian recursive (Kalman) smoother, which also provides an improved estimate of uncertainty (Wallis et al., 2023b).

After filtering and smoothing, time series data were spatially averaged across 3 x 3 km sample regions manually placed on each glacier, to calculate a single time series for each location in the study. This box size ensured adequate coverage while avoiding potential interference from border regions. For all glaciers, one measurement location was positioned approximately 1 km inland of the grounding line to ensure placement on grounded ice. The grounding line was sourced from Wallis et al. (2024), who provided the most recent dataset covering the entire study region. Additional measurement locations were placed on grounded ice for larger glaciers to improve spatial coverage, paying particular attention to both main and side streams. For glaciers with floating tongues, measurement locations were also positioned on floating ice to capture the dynamics of glacier flow more comprehensively. However, since most of the floating tongues broke off at some point during the analysis, these squares often did not cover the full ten-year period. Therefore, the data of floating measurement locations were only used to complement the analyses of their respective glaciers and were removed from analyses where only full time series were used (ice velocity trend analysis, seasonality analysis, and correlation analysis).

https://doi.org/10.5194/egusphere-2025-5492
Preprint. Discussion started: 15 December 2025

Table 2. Window and step sizes in pixels used for offset tracking of SAR images.

Window Range	Window Azimuth	Step Range	Step Azimuth
256	64	60	16
362	144	86	32
400	160	100	40
192	48	48	12
244	56	56	14
256	64	64	16
288	72	72	18
320	80	80	20

3.3 Seasonality analysis

Prior to the seasonality analysis, gaps in the monthly terminus area records, which primarily occurred during polar night, were linearly interpolated based on the closest preceding and following observations to ensure a continuous input time series. While there are more sophisticated gap filling approaches, linear interpolation provides a statistically straight-forward way to bridge recurring gaps and has been previously used for this purpose in other glacier front studies (Moon et al., 2024; KC et al., 2025; Li et al., 2024; York et al., 2020). To analyse intra-annual flow dynamics, the Seasonal and Trend decomposition using Loess (STL) methodology of Cleveland et al. (1990) was applied to decompose the monthly time series into three components: trend, seasonal, and remainder. Following the STL decomposition, the seasonality strength (F_S) was derived using the following formula, also developed by Cleveland et al. (1990):

$$F_S = \max\left(0.1 - \frac{Var(R_t)}{Var(S_t + R_t)}\right) \quad (1),$$

where $Var(R_t)$ is the variance of the remainder component and $Var(S_t + R_t)$ is the combined variance of the seasonal and remainder components. A low F_S indicates minimal seasonality, while F_S close to 1 suggests strong seasonal behaviour, as the variance of R_t is negligible compared to $S_t + R_t$. For each glacier, (F_S) was calculated for both the ice surface velocity time series and terminus area data. Glaciers with $F_S > 0.2$ were considered as exhibiting significant seasonality and were selected for further analysis. For these glaciers, time series were resampled into seasonal medians (spring: Sep–Nov, summer: Dec–Feb, autumn: Mar–May, winter: Jun–Aug), yielding four values per year to assess seasonal patterns and the timing of maximum and minimum changes.

3.4 Correlation analysis

To examine the relationship between ice surface velocity dynamics and terminus area changes, a lagged cross-correlation analysis was conducted. By shifting one time series relative to the other and identifying the lag at which the strongest correlation occurred, insights can be gained into whether terminus area changes preceded or followed velocity variations. The methodological framework was derived from Ultee et al. (2022), who used normalized cross-correlation to study the influence

https://doi.org/10.5194/egusphere-2025-5492
Preprint. Discussion started: 15 December 2025

of terminus position changes on velocity variability at Helheim Glacier, among other aspects. First, the time series were tested for stationarity by applying the Dickey-Fuller (Dickey and Fuller, 1979) and KPSS (Kwiatkowski et al., 1992) tests. To address any non-stationarity and reduce the impact of long-term trends, first-order differencing was applied to each time series. The time series were then merged, retaining NaN values to ensure correct shifting of the lags during the cross-correlation computations. Normalized cross-correlations were computed across lags ranging from –24 to +24 months, representing approximately 25 % of the time series length when NaN values were removed, ensuring sufficient overlapping data points. To account for autocorrelation within the time series, which can lead to spurious correlations, the statistical significance at the 95 % confidence level was evaluated. This was accomplished by applying lag-specific significance thresholds corrected for autocorrelation following the methodology of Dean and Dunsmuir (2016). Lastly, we identified the largest magnitude statistically significant correlation for each measurement location, along with the corresponding lag in months at which that extreme value occurred.

4 Results

4.1 Terminus area changes

Our observations show that most glaciers experienced significant ice area loss, with retreat rates strongly varying across the peninsula (Fig. 2a). By 2023, the cumulative terminus area of all 42 glaciers had decreased by approximately 278.89 km^2 compared to their extent in 2013. Glaciers on the eastern side accounted for the majority of this loss, contributing 202.99 km^2 (73 %), while the 30 glaciers on the western side retreated 75.91 km^2 (27 %). The most pronounced retreat was observed among glaciers in the Larsen A and Larsen B embayments on the eastern coast. There, the HGE Glacier system alone lost 139.63 km^2 of ice, followed by the DBE Glacier complex with 32.38 km^2. Other notable terminus area declines included Akaga-Sinion (–13.55 km^2) and Crane (–7.1 km^2). Most glaciers in these two embayments initially advanced before retreating sharply, marked by a distinct change point. In Larsen B, all glaciers advanced between 2013 and the end of 2021, followed by pronounced calving events and rapid retreat beginning in early 2022. In Larsen A, all glaciers reached their maximum extent during the eleven-year observation period in 2016 (2017 for DBE). After this, a continuous, albeit less uniform, retreat began. On the western side, only few glaciers experienced retreat of comparable magnitude. The most substantial change occurred at Prospect Glacier in Wordie Bay, which lost 51.84 km^2 between April and October 2018. In subsequent years, the glacier showed signs of recovery, with a gradual advance becoming evident. Most other western glaciers showed minimal terminus changes, ranging between –1 km^2 and 1 km^2. The only glacier that experienced a substantial net expansion in 2023 was Fleming Glacier, which gained 9.29 km^2 relative to its 2013 extent. However, Fleming Glacier's terminus area dynamics were characterized by multi-year fluctuations, rather than a consistent trend of advance. Overall, western glaciers exhibited more heterogeneous behaviour with no clear regional pattern becoming evident. About half retreated steadily, seven displayed fluctuating but trendless dynamics, and only four showed slight signs of advance – all located along the norther section of the western coast.

https://doi.org/10.5194/egusphere-2025-5492
Preprint. Discussion started: 15 December 2025

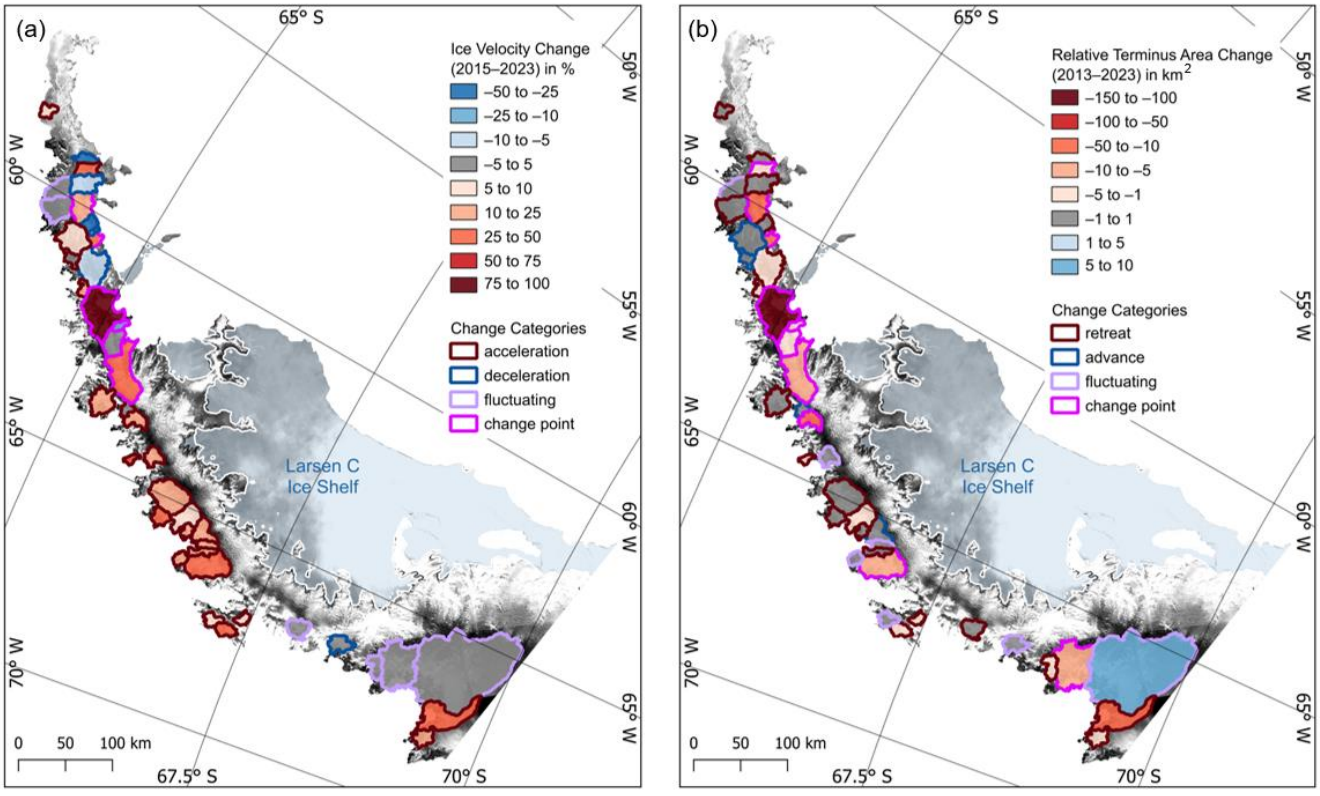

Figure 2 Spatial distribution of (a) ice velocity change (in %) between the annual means of 2015 and 2023, and (b) terminus area changes between 2013 and 2023 across the AP. Both panels include a classification of temporal variation patterns derived from the time series. The change categories are described in Table 1 and example dynamics for the "change point" category are illustrated in Figure 3. Background: Sentinel-1 (ESA), ADD coastline v7.10 (Gerrish et al., 2024), grounding line (Wallis et al., 2024).

4.2 Ice surface velocity

The ice surface velocity analysis revealed a distinct east-west divide in the magnitude of flow speeds across the AP. On the western side, most glaciers exhibited significantly higher velocities with median flow speeds ranging from 500 m yr^{-1} to over 1000 m yr^{-1}, while on the eastern side median velocities ranged from 100 m yr^{-1} to 500 m yr^{-1}. The highest flow speeds were recorded at Fleming Glacier in Wordie Bay, where median velocities reached 2,278 m yr^{-1}. Over the ten-year period approximately 71 % of the glaciers accelerated, with an average velocity increase of 10 % (94 m yr^{-1}) (Fig. 2b). Along the western coast, most glaciers experienced a continuous increase in ice flow speeds, with the most significant accelerations occurring at Cadman and Prospect Glaciers. Prospect Glacier's grounded ice on the middle flow unit experienced a speedup of 93 % between the 2018 and 2021, rising from 649 m yr^{-1} to 1252 m yr^{-1}. However, its two other flow units showed only slight positive trends over the entire study period. During the same time, the grounded ice at Cadman Glacier accelerated, but by a more modest 36 %. In contrast, the velocity of its floating tongue more than doubled within twelve months starting in November 2019 and rising from 1,090 m yr^{-1} to 2,412 m yr^{-1}, before it calved off (Wallis et al., 2023a). Despite this widespread

https://doi.org/10.5194/egusphere-2025-5492
Preprint. Discussion started: 15 December 2025

pattern of increasing flow speeds, not all western glaciers experienced acceleration. In the southernmost part in and around Wordie Bay, and the northern tip glaciers displayed mostly fluctuating dynamics or slight trends of deceleration.

On the eastern side, a general decline in flow speeds was observed, particularly in the first years of the study period. Glaciers in the Larsen B embayment showed a consistent slowdown throughout most of the study period, followed by a significant acceleration starting in early 2022 (Surawy-Stepney et al., 2024), which continued through to February 2024 (Fig. 3). During this period, the grounded measurement locations of HGE Glaciers main flow unit sped up by approximately 145 %. Similarly, at Crane Glacier, the velocity of the grounded ice doubled, resulting in an increase of 619 m yr^{-1}. The floating tongues of both glaciers collapsed in early 2022, hence no floating ice velocity measurements after the calving events were available. In contrast, flow speeds of glaciers in the neighbouring Larsen A embayment showed significant variability, clearly differing from the unique dynamics observed in Larsen B.

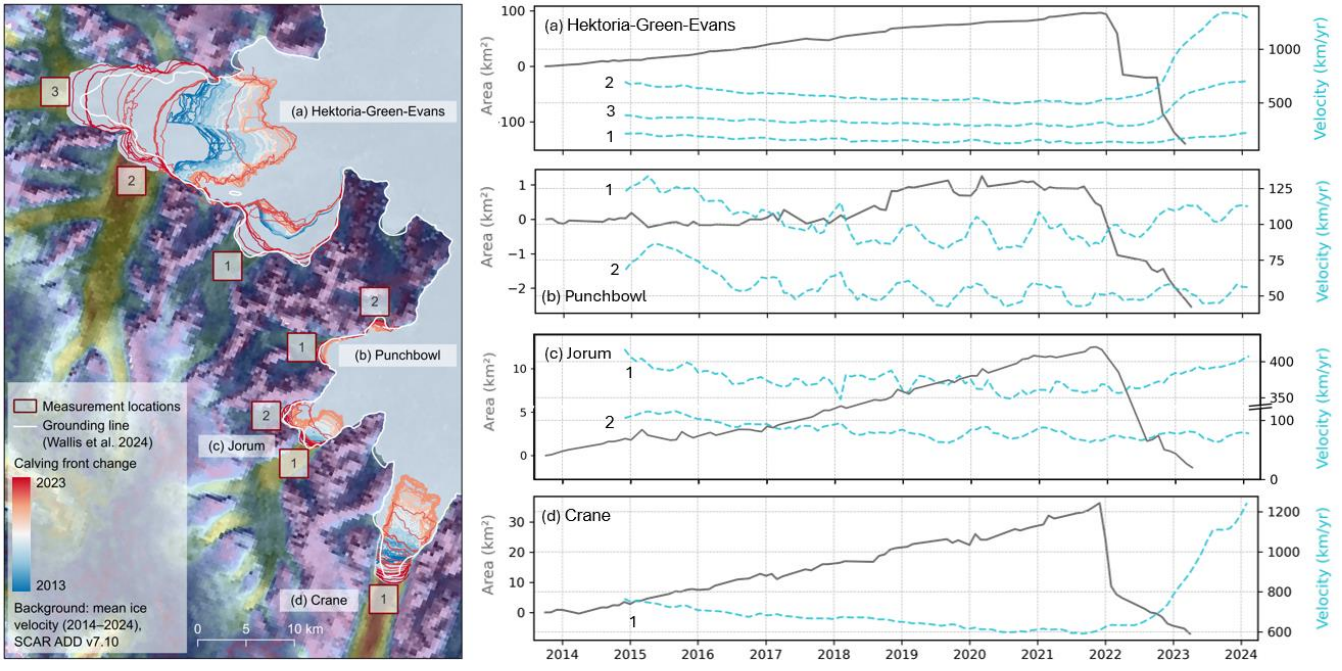

Figure 3 Monthly time series of glacier terminus area change and grounded ice velocity for glaciers in the Larsen B embayment from 2013 to 2024. For HGE, Punchbowl, and Jorum Glaciers additional measurement locations were placed on grounded ice to ensure adequate coverage. The measurement locations along with color-coded calving front locations for Larsen B glaciers area depicted on the map on the left. The records highlight uniform glacier dynamics in the embayment, characterized by an initial phase of advance/ slowdown that changes into retreat and acceleration. In addition, these plots illustrate dynamics typical for glaciers of the category "change point" in Figure 2, which has been described in Table 1.

4.3 Relationship between terminus area and ice surface velocity

To investigate the relationship between ice surface velocity dynamics and terminus area changes, a lagged cross-correlation analysis was conducted. The results presented in Figure 4c provide a glacier-level overview of the correlation strength between the two variables. It should be noted that for most glaciers the results presented here do not distinguish between positive and

https://doi.org/10.5194/egusphere-2025-5492
Preprint. Discussion started: 15 December 2025

negative correlations, nor do they specify the lag at which maximum correlation occurred, as this would go beyond the scope of this study. These detailed results, along with all measurements from the ice velocity, terminus area change, and seasonality analysis are available in the supplements. The findings show that for most glaciers, correlation between the two variables ranged from non-significant/weak in 43 % of the cases to moderate for half of the glaciers, with those in the northern part of the study region generally exhibiting slightly higher correlation coefficients. The highest values, ranging from 0.6 to 0.8, were observed for Malorad, HGE, and Vallot Glaciers. Of these, HGE in the Larsen B embayment demonstrated particularly strong interconnected dynamics, with negative correlations of -0.8 and -0.76 at its two grounded measurement locations. There, terminus area changes consistently led velocity changes within a timeframe of eight to twelve months. Similarly, at Malorad Glacier in the north terminus area changes led velocity variations with a correlation of –0.64 and a lag of 22 months. In contrast, at Vallot Glacier further south terminus area lagged ice velocity dynamics with a correlation of 0.62 and a lag of 10 months.

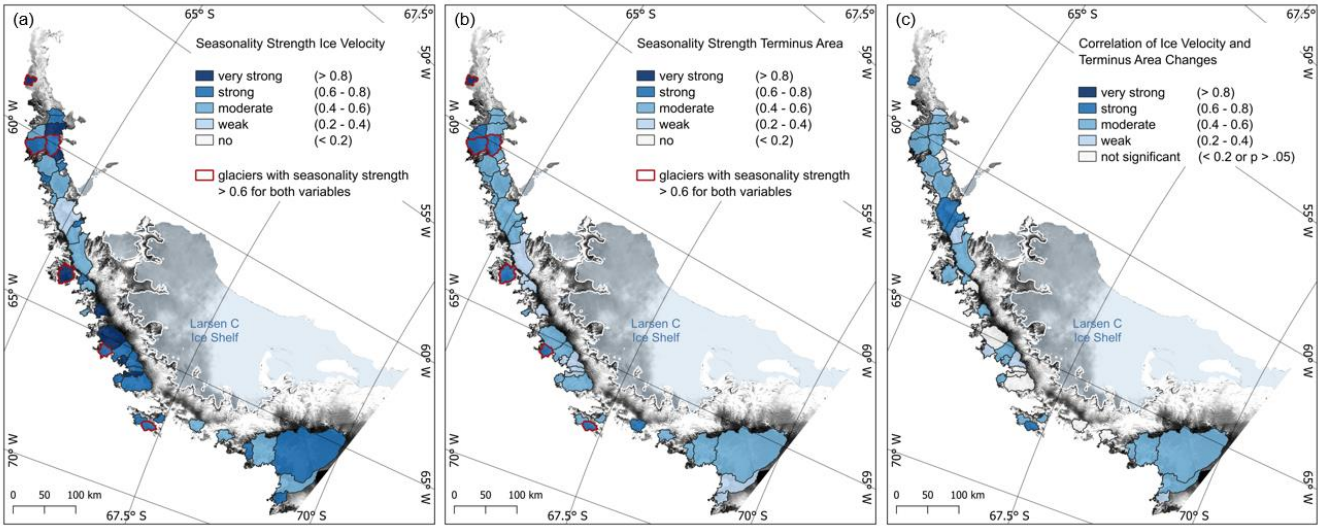

Figure 4 Spatial patterns of seasonality statistics for (a) terminus area changes and (b) ice velocity dynamics, which ranged from very strong to no seasonality. Red outlines mark glaciers with strong seasonal patterns for both variables. (c) Glacier drainage basins shaded by correlation statistics of monthly ice velocity and terminus area variations ranging from very strong to not significant, which is characterized by correlations below 0.2 and/ or p > 0.05. Background: Sentinel-1, ESA, ADD coastline v7.10 (Gerrish et al., 2024), grounding line (Wallis et al., 2024).

4.4 Seasonality Analysis

To gain deeper insights into intra-annual glacier dynamics, we analysed the seasonality strength of terminus area (Fig. 4a) and ice velocity changes (Fig. 4b). Our observations show that seasonal variability is widespread among the 42 investigated glaciers. All ice velocity time series, except those of HGE Glacier system, exhibited F_S values greater than 0.4, with 67 % of glaciers showing strong ($F_S > 0.6$) to very strong ($F_S > 0.8$) seasonality. The most pronounced seasonal patterns were observed for Trooz (0.93), Birley (0.93), and McCane (0.89) Glaciers, all situated in Darbel Bay in the middle of the western coast. Additional glaciers exhibiting very strong seasonality were Malorad, Hugi, Hopkins, DBD, and Pyke, all of which also demonstrated seasonality strength values between 0.6 and 0.8 and were mostly located on the northern half of the AP. For

https://doi.org/10.5194/egusphere-2025-5492
Preprint. Discussion started: 15 December 2025

most glaciers, peak ice surface velocities were observed during the summer months, with some glaciers reaching maximum speeds slightly earlier in late spring or slightly later in early autumn. Minimum velocities typically occurred in winter, occasionally extending into early spring. However, a few glaciers showed atypical seasonal dynamics. Boydell, Heim, and Zaychar exhibited peak velocities in spring, while Funk reached its maximum flow speed during winter. Minimum velocities for these glaciers were reached during the summer months.

For terminus area changes, seasonal variability was widespread as well, with 52 % of the glaciers exhibiting a moderate seasonal component and 19 % strong seasonality. However, the average F_S for terminus area changes was generally 0.19 lower than that observed for ice surface velocity and for twelve of 42 glaciers a seasonality strength below 0.4 was found. Regionally, glaciers at the norther tip of the peninsula displayed the strongest seasonal patterns, but $F_S > 0.6$ was also found for several individual glaciers along the western coast. The highest F_S was observed for Malorad (0.86) and DBE (0.79) Glaciers, both located at the northern tip. These glaciers not only exhibited strong seasonal patterns in their terminus area changes but also showed similarly high seasonality in their ice velocity dynamics. Other glaciers that displayed high seasonality for both variables (terminus area F_S 0.61–0.69; ice velocity F_S 0.76–0.93) included Stringfellow, Trooz, Keith, and Vallot.

5 Discussion

5.2 Long-term trend of glacier retreat

Over the ten-year study period (2013–2023), 31 out of the 42 investigated glaciers (74 %) underwent terminus area loss. This observation is consistent with previous studies (Cook et al., 2014; Kang et al., 2024; Seehaus et al., 2018; Silva et al., 2020), which taken together cover the period from 1940 to 2015 and consistently report widespread glacier retreat, highlighting the persistence of a long-term trend of ice loss on the AP. Despite this overall trend, a clear spatial disparity in retreat magnitude emerged between the eastern and western coasts. The twelve glaciers on the eastern side lost a total of 202.99 km^2, while the 30 glaciers on the western side lost 75.91 km^2. A similar imbalance was reported by Seehaus et al. (2018), who in their long-term analysis (1985–2015), found a 5.7 % area loss (208.59 km^2) for eastern glaciers compared to only 0.2 % (9.14 km^2) in the west, based on a larger glacier sample. These findings suggest an acceleration of ice loss, particularly along the western coast, which is supported by our observation that 60 % of western glaciers underwent consistent terminus retreat. On the eastern side, the largest losses occurred in the Larsen B embayment, where glaciers retreated by 150.61 km^2 initiated by major calving events in early 2022, after eight years of continuous terminus advance. These dynamics have been described and investigated in several recent studies (Surawy-Stepney et al., 2024; Sun et al., 2023; Fluegel and Walker, 2024; Ochwat et al., 2024), which reported retreat comparable to our findings. Although the landfast sea ice in the embayment was not thick enough to directly buttress the flow of grounded ice, it consolidated the ice front during its persistence and its sudden breakup in January 2022 likely triggered the near-synchronous onset of calving (Ochwat et al., 2024; Fluegel and Walker, 2024; Surawy-Stepney et al., 2024). The drivers of the ongoing retreat remain debated, but it is unlikely that a single factor was responsible. Instead, a combination of structural weakening, loss of buttressing, and ocean forcing likely amplified retreat, resulting in the

https://doi.org/10.5194/egusphere-2025-5492
Preprint. Discussion started: 15 December 2025

observed ice loss (Surawy-Stepney et al., 2024; Fluegel and Walker, 2024; Ochwat et al., 2024). Conversely, on the western side of the peninsula continuous and steady terminus retreat of a smaller magnitude dominated, suggesting comparatively stable behaviour of glacier termini along the western coast relative to those in the east. This observation is consistent with Cook et al. (2016), who attributed the smaller magnitude of frontal changes in this region to the relatively cold ocean temperatures (approximately -1.8°C) of the Bransfield Strait (Cook et al., 2016; Dryak and Enderlin, 2020). A further contributing factor is the steeply sloping bed topography on the western side, which restricts the formation of extensive floating tongues and results in glaciers calving at or close to their grounding line, thereby making them less susceptible to large terminus retreat. An exception to this pattern was found in Wordie Bay, the southernmost part of the study region, where glaciers displayed pronounced fluctuations (Fleming) and large-scale calving (Prospect). Although no recent studies have specifically examined the terminus dynamics of glaciers in Wordie Bay, our findings are supported by Friedl et al. (2018) and Dømgaard et al. (2025), who reported substantial grounding line retreat since the 1960s (Fleming ~13 km, Carlson ~6.6 km, Prospect ~2.5 km) in the region alongside significant increases in thinning rates in recent years. These results indicate that, more than three decades after the partial disintegration of the Wordie Ice Shelf, glaciers in the embayment remain far from being in a stable state. In this sector of the AP, the cooling influence of the Bransfield Strait likely diminishes and glacier dynamics appear to be governed by the warmer waters of the Bellingshausen Sea, which has undergone significant warming since the early 2000s (Cook et al., 2016). This warming, in combination with increased upwelling of circumpolar deep water (CDW), has already been linked to the frontal retreat of tidewater glaciers in this region (Friedl et al., 2018; Cook et al., 2016). Furthermore, variability in sea ice extent (SIE) seems to have played an important role, as years of record-low SIE coincided with phases of enhanced calving and glacier retreat in the embayment (Josey et al., 2024; Purich and Doddridge, 2023). In sum, these patterns show that along the western coast regional differences in ocean temperature regime and CDW access as well as sea-ice variability govern terminus area changes and account for the observed regional variability of glacier dynamics.

5.2 Long-term trend of glacier acceleration

Over the ten-year study period, grounded measurement locations across the 42 glaciers in the study region exhibited an average velocity increase of 10 % (94 m yr^{-1}), supporting previous findings (Seehaus et al., 2018; Davison et al., 2024) and indicating a multi-decadal trend of accelerating ice flow on the AP since 1985. Significant increases in ice flow speed were mainly observed for glaciers south of 65° S, while glaciers in the northern part of the study region exhibited more variable behaviour, showing fluctuations without consistent trend or even signs of deceleration – particularly on the eastern side. These patterns contrast with findings of Seehaus et al. (2018), who reported velocity increases of 41–44 % for northern AP glaciers from 1985 to 2015. Our results suggests that the rate of acceleration in this region has slowed since then, with glaciers in the Larsen A, Larsen Inlet, and Prince Gustav embayments showing decelerations of 15–33 %. The spatial distribution of velocity trends largely mirrors the patterns of terminus area change, indicating that both dynamics were likely influenced by similar external drivers. Specifically, recent ocean warming in the Bellingshausen Sea appears to have driven the observed acceleration along the southern and central western coast, while colder water masses from the Weddell Sea exerted a stabilizing influence on

https://doi.org/10.5194/egusphere-2025-5492
Preprint. Discussion started: 15 December 2025

glacier dynamics in the eastern and northwestern regions (Shen et al., 2018; Dryak and Enderlin, 2020; Cook et al., 2016). The most pronounced short-term acceleration on the western coast was found for Cadman Glacier, where flow speeds at the floating tongue increased by 121 % (36 % on grounded ice) within just twelve months, starting in November 2016. This observation is consistent with findings from Wallis et al. (2023a) and aligns with Davison et al. (2024), who observed that acceleration is strongest at glaciers connected to deep, cross-shelf troughs that channel warm water toward their base. At Cadman, a 400 m deep channel enabled the intrusion of warm CDW, leading to persistent thinning and ungrounding from a bedrock ridge (Wallis et al., 2023a), which likely triggered this rapid acceleration. This reinforces the importance of glacier- and region-specific factors, such as fjord depth, basin geometry, and subglacial conditions, in modulating ice flow responses to ocean forcing, as previously emphasized by Seehaus et al. (2018). The largest accelerations across the entire study area were observed in the Larsen B embayment, where glacier velocity dynamics also differed markedly from those in the other regions. After a prolonged slowdown during the first eight years, which was likely part of a longer term restabilisation following the post-ice shelf collapse dynamic activation – with calving rates dampened by the presence of sea ice and mélange (Rott et al., 2018) – glaciers began accelerating sharply in early 2022 continuing through February 2024. The most pronounced changes occurred at the HGE Glacier system, where grounded ice velocity increased by approximately 145 %, and at Crane Glacier, which nearly doubled in speed. The timing and magnitude of these dynamics are consistent with previous studies (Ochwat et al., 2024; Surawy-Stepney et al., 2024; Fluegel and Walker, 2024), which identified the collapse of fast ice and the subsequent large calving events as the primary drivers. The ongoing acceleration was likely amplified by long-term thinning, oceanic variability, and short-term triggers such as atmospheric river induced surface melt and ocean swell activity (Fluegel and Walker, 2024; Parsons et al., 2024; Surawy-Stepney et al., 2024). The only notable divergence comes from Sun et al. (2023), who reported no immediate speedup – likely because their velocity time series ended in August 2022, before the most substantial acceleration occurred.

5.3 Seasonal changes in ice speed and terminus area

Seasonal variations in ice surface velocity were widespread: all glaciers exhibited at least moderate seasonality, and 67 % showed strong to very strong intra-annual fluctuations. Seasonality was strongest in the central and northern regions and less pronounced around the Larsen B embayment. Our findings align with those of Wallis et al. (2023b), who reported a mean summer speedup of over 10 % on 76 of the 105 glaciers they studied along the western coast, with the strongest increases in flow speed occurring at norther latitudes. Although direct comparison is limited by differences in methodology and glacier selection, the overall trends are consistent with our findings. For eastern glaciers, Tuckett et al. (2019) suggested that surface meltwater drainage might be a driver of summertime speed-up, although there is evidence to suggest that this region was not grounded at the time of the discharge event which alters the processes available to drive change (Rott et al., 2020). Future work will help establish the relative importance of surface meltwater as a lubricant for ice flow on the AP, particularly in the context of a warming climate where surface melt is expected to increase. The weaker seasonal velocity signals on Larsen B glaciers are in part likely to be caused by the persistence of landfast sea ice in the embayment, which has been shown to

https://doi.org/10.5194/egusphere-2025-5492
Preprint. Discussion started: 15 December 2025

consolidate glacier termini and dampen iceberg calving frequency (Amundson et al., 2010; Robel, 2017). However, seasonal variability will also be impacted by the smaller ocean temperature anomaly in the cold Weddell Sea (Wallis et al., 2023b), relative to the warmer Bellingshausen Sea on the west, which provides an environmental driver for the observed regional differences in the seasonality.

For terminus area dynamics, annual cycles were present but generally less pronounced, with 19 % of the glaciers exhibiting strong and 52 % moderate seasonality. As with ice velocity, stronger seasonal signals were observed at the northern tip but also at several individual glaciers along the western coast. These glaciers shared the characteristic of terminating directly into the open ocean rather than being located within sheltered embayments. At first glance, these results appear to contrast with Wallis et al. (2023b), who reported seasonal patterns in all eight calving front time series they analysed. However, when comparing individual glaciers the findings align. Both studies identified strong seasonality at Trooz and Keith Glaciers, and the seasonal patterns they observed for Fleming Glacier were also evident in our data. On Cadman Glacier we only detect a weak seasonal component, which is not as large as on other glaciers in the region. Finally, the overall lower strength of the seasonality in terminus area change in our dataset may be partly explained by 14-week gaps from May to mid-August during polar night, which remove information for the entire winter season and likely weaken the seasonal signal. While terminus advance during winter is in most cases still evident in spring, potential winter dynamics are not captured, as the gaps were filled using linear interpolation to avoid introducing spurious variability or artificial seasonal patterns. To date, no studies have conducted a comprehensive analysis of seasonal variations in terminus dynamics of AP glaciers, leaving the mechanisms controlling intra-annual terminus fluctuations largely speculative. Insights from Moon et al. (2015) indicate a strong relationship between the seasonal presence and breakup of sea ice/mélange and terminus change of tidewater glaciers in Greenland, suggesting that sea ice-free periods and reduced rigid mélange may similarly influence AP glaciers. This hypothesis is supported by our observation that glaciers outside sheltered embayments exhibited stronger seasonal signals, as these glaciers are likely more directly exposed to sea-ice variability and open-ocean conditions. Additionally, seasonal variations in ocean temperature and enhanced surface runoff during the summer months (Wallis et al., 2023b) may further modulate terminus fluctuations, potentially acting jointly with mélange conditions to shape intra-annual glacier behaviour.

5.4 Correlation between terminus area changes and ice velocity dynamics

Half of the investigated glaciers exhibited correlations of moderate strength between terminus area changes and ice surface velocity. For around 43 % the correlation between the two variables was either non-significant or below 0.2 and only three glaciers showed strongly interconnected dynamics. These results suggest that, for most glaciers in the study region, terminus area changes and ice velocity dynamics were largely independent of one another. This is consistent with findings from Ultee et al. (2022), Moon et al. (2015), and Davidson et al. (2020), who reported similarly weak relationships between these two variables for different glaciers in Greenland, noting that on seasonal to interannual timescales ice speed is more strongly linked to surface-derived meltwater inputs. While these studies are not directly transferable to the AP due to different glaciological settings, they provide a useful point of comparison, particularly in light of the limited research on this relationship for glaciers

https://doi.org/10.5194/egusphere-2025-5492
Preprint. Discussion started: 15 December 2025

in our study area. Ultee et al. (2022) suggested that the sensitivity of surface velocity to terminus position depends on whether the glacier terminus approached a critical threshold. If such a position is reached during the observation period, changes in terminus position may exert a strong influence on ice flow, resulting in higher correlations. This hypothesis is supported by our findings for the HGE Glacier system, where we observed strong negative correlations (-0.76 to -0.8) at a lag of eight to twelve months, with terminus area changes preceding changes in velocity. It is likely that HGE's terminus reached such a threshold during its eight-year period of pronounced advance, amplifying the impact of its dynamics on upstream flow changes. For Malorad and Vallot Glaciers, where correlations exceeded 0.6, there was no indication that termini reached a comparable critical state, as both glaciers have been retreating continuously. In these cases, high correlations are more likely explained by shared seasonal patterns. At Malorad Glacier, the strongest correlation occurred at a lag of 22 months, but secondary peaks at 4, 10, and 16 months in the correlogram suggest that first-order differencing was insufficient to fully remove seasonal autocorrelation. A similar pattern was observed for Vallot Glacier, further indicating that the apparent relationship between terminus area and velocity at these sites likely reflected underlying seasonal cycles rather than causal interaction.

6 Conclusion

Our analysis builds upon earlier work (Kang et al., 2024; Ochwat et al., 2024; Rott et al., 2018; Seehaus et al., 2018; Seehaus et al., 2015; Wallis et al., 2023b; Wallis et al., 2023a) by either extending the study period, broadening the regional coverage, or providing observations at higher temporal resolution. Sub-seasonal records of terminus area (2013–2023) and ice flow speed (2014–2024) reveal widespread patterns of glacier retreat and acceleration but also highlight pronounced spatial and temporal variability. These results underscore the importance of temporally detailed observation of glaciological change across AP outlets, which often respond to environmental forcing on timescales of days to months, as exemplified by the near-immediate onset of calving of Larsen B glaciers following the collapse of landfast sea ice.

The sub-seasonal terminus area records also enabled the first comprehensive seasonality analysis for most of the studied glaciers, extending the work of Wallis et al. (2023b), who previously analysed only eight selected basins along the western coast. We found that seasonal patterns in both flow speed and terminus area change were widespread, with the seasonal signals generally more pronounced in ice velocity. The underlying causes of the observed differences in seasonality strength, as well as the drivers of seasonal terminus dynamics, remain an open question, highlighting the need for future research to identify region- and basin-specific controls of seasonal variability. This becomes particularly relevant given the extremely low Antarctic sea ice cover in recent years (Purich and Doddridge, 2023), the projected atmospheric warming of 0.5–1.5°C (2°C in autumn and winter), as well as the intensification of the Southern Ocean warming (Cai et al., 2023), all of which are likely to further amplify the seasonal variability of glaciers on the AP.

Finally, we found weak to moderate correlations between ice velocity dynamics and terminus area changes. While not generally considered strong, these correlations were mostly significant and higher than those reported in previous studies for glaciers in Greenland, which consistently identified runoff as the primary control on ice velocity variability. Our findings suggest that the

https://doi.org/10.5194/egusphere-2025-5492
Preprint. Discussion started: 15 December 2025

relationship between flow speed and terminus dynamics warrants further investigation. Future work should expand this analysis to include additional processes such as runoff and thinning, while also accounting for environmental and geometric controls, in order to better disentangle their roles in shaping the long-term evolution of AP glaciers.

Data availability

Calving front positions and terminus data are publicly available at PANGEA (doi: 10.1594/PANGAEA.963725); documentation is provided in Loebel et al. (2025). The original Copernicus Sentinel-1A/B data supporting this study can be downloaded from the Copernicus Data Space Ecosystem (https://dataspace.copernicus.eu/). Surface velocity fields are available from the authors upon request. Please contact author A.E.H. or R.S. for this purpose. Glacier outlines and coastline polygons were obtained from the Antarctic Digital Database (https://www.add.scar.org/). Bedrock topography was derived from Bedmap3 (British Antarctic Survey; doi: 10.5285/2d0e4791-8e20-46a3-80e4-f5f6716025d2).

Author contribution

Conceptualization: S.L.; C.A.B. Data curation: S.L.; C.A.B.; R.A.W.S.; A.E.H. Formal Analysis: S.L. Funding Acquisition: C.A.B.; Investigation: S.L. Methodology: S.L.; R.A.W.S. Project administration: C.A.B. Supervision: C.A.B.; R.A.W.S.; A.E.H. Validation: S.L. Visualization: S.L. Writing – original draft: S.L.; R.A.W.S.; Writing – review and editing: C.A.B.; R.A.W.S.; A.E.H. All authors approved the final submitted draft.

Competing interest

The authors declare that they have no conflicts of interest.

Acknowledgements

The authors gratefully acknowledge the European Space Agency and the European Commission for the acquisition, generation, and availability of Copernicus Sentinel-1 data. Ice velocity data processing was undertaken on ARC4 and AIRE, part of the high-performance computing facilities at the University of Leeds, UK. R.A.W.S. is funded by the Natural Environment Research Council (NERC) SENSE Centre for Doctoral Training (NE/T00939X/1). A.E.H. is supported by ESA through the 5D Antarctica project (4000146702/24/I-KE). S.L. is supported by the Deutsche Forschungsgemeinschaft (DFG, German Research Foundation) in the context of the DFG Research Unit 5696, “SOS: Serverless Scientific Computing and Engineering for Earth Observation and Sustainability Research” (project number: 522760169; https://dfg-sos.de/, accessed on 04 November 2025).

https://doi.org/10.5194/egusphere-2025-5492
Preprint. Discussion started: 15 December 2025

References

Amundson, J. M., Fahnestock, M., Truffer, M., Brown, J., Lüthi, M. P., and Motyka, R. J.: Ice mélange dynamics and implications for terminus stability, Jakobshavn Isbræ, Greenland, JGR Earth Surface, 115, https://doi.org/10.1029/2009JF001405, 2010.

Baumhoer, C. A., Dietz, A. J., Dech, S., and Kuenzer, C.: Remote Sensing of Antarctic Glacier and Ice-Shelf Front Dynamics—A Review, Remote Sensing, 10, 1445, https://doi.org/10.3390/rs10091445, 2018.

Cai, W., Gao, L., Luo, Y., Li, X., Zheng, X., Zhang, X., Cheng, X., Jia, F., Purich, A., Santoso, A., Du, Y., Holland, D. M., Shi, J.-R., Xiang, B., and Xie, S.-P.: Southern Ocean warming and its climatic impacts, Science bulletin, 68, 946–960, https://doi.org/10.1016/j.scib.2023.03.049, 2023.

Carrasco, J. F. and Cordero, R. R.: Analyzing Precipitation Changes in the Northern Tip of the Antarctic Peninsula during the 1970–2019 Period, Atmosphere, 11, 1270, https://doi.org/10.3390/atmos11121270, 2020.

Carrasco, J. F., Bozkurt, D., and Cordero, R. R.: A review of the observed air temperature in the Antarctic Peninsula. Did the warming trend come back after the early 21st hiatus?, Polar Science, 28, 100653, https://doi.org/10.1016/j.polar.2021.100653, 2021.

Cleveland, R. B., Cleveland William S., McRae, J. E., and Terpenning, I.: STL: A seasonal trend decomposition preocedure based on Loess, Journal of Official Statistics, 6, 3–73, available at: https://www.wessa.net/download/stl.pdf, 1990.

Cook, A. J. and Vaughan, D. G.: Overview of areal changes of the ice shelves on the Antarctic Peninsula over the past 50 years, The Cryosphere, 4, 77–98, https://doi.org/10.5194/tc-4-77-2010, 2010.

Cook, A. J., Holland, P. R., Meredith, M. P., Murray, T., Luckman, A., and Vaughan, D. G.: Ocean forcing of glacier retreat in the western Antarctic Peninsula, Science (New York, N.Y.), 353, 283–286, https://doi.org/10.1126/science.aae0017, 2016.

Cook, A. J., Vaughan, D. G., Luckman, A. J., and Murray, T.: A new Antarctic Peninsula glacier basin inventory and observed area changes since the 1940s, Antartic science, 26, 614–624, https://doi.org/10.1017/S0954102014000200, 2014.

Cook, A. J., Fox, A. J., Vaughan, D. G., and Ferrigno, J. G.: Retreating glacier fronts on the Antarctic Peninsula over the past half-century, Science (New York, N.Y.), 308, 541–544, https://doi.org/10.1126/science.1104235, 2005.

Davison, B. J., Sole, A. J., Cowton, T. R., Lea, J. M., Slater, D. A., Fahrner, D., and Nienow, P. W.: Subglacial Drainage Evolution Modulates Seasonal Ice Flow Variability of Three Tidewater Glaciers in Southwest Greenland, JGR Earth Surface, 125, https://doi.org/10.1029/2019JF005492, 2020.

Davison, B. J., Hogg, A. E., Slater, T., Rigby, R., and Hansen, N.: Antarctic Ice Sheet grounding line discharge from 1996–2024, Earth Syst. Sci. Data, 17, 3259–3281, https://doi.org/10.5194/essd-17-3259-2025, 2025.

https://doi.org/10.5194/egusphere-2025-5492
Preprint. Discussion started: 15 December 2025

Davison, B. J., Hogg, A. E., Moffat, C., Meredith, M. P., and Wallis, B. J.: Widespread increase in discharge from west Antarctic Peninsula glaciers since 2018, The Cryosphere, 18, 3237–3251, https://doi.org/10.5194/tc-18-3237-2024, 2024.

Dean, R. T. and Dunsmuir, W. T. M.: Dangers and uses of cross-correlation in analyzing time series in perception, performance, movement, and neuroscience: The importance of constructing transfer function autoregressive models, Behavior research methods, 48, 783–802, https://doi.org/10.3758/s13428-015-0611-2, 2016.

Dickey, D. A. and Fuller, W. A.: Distribution of the estimators for autoregressive time series with a unit root, Journal of the American statistical association, 74, 427–431, 1979.

Doake, C. S. M. and Vaughan, D. G.: Rapid disintegration of the Wordie Ice Shelf in response to atmospheric warming, Nature, 350, 328–330, https://doi.org/10.1038/350328a0, 1991.

Dømgaard, M., Millan, R., Andersen, J. K., Scheuchl, B., Rignot, E., Izeboud, M., Bernat, M., and Bjørk, A. A.: Half a century of dynamic instability following the ocean-driven break-up of Wordie Ice Shelf, Nature communications, 16, 4016, https://doi.org/10.1038/s41467-025-59293-1, 2025.

Dong, Y., Zhao, J., Floricioiu, D., Krieger, L., Fritz, T., and Eineder, M.: High-resolution topography of the Antarctic Peninsula combining the TanDEM-X DEM and Reference Elevation Model of Antarctica (REMA) mosaic, The Cryosphere, 15, 4421–4443, https://doi.org/10.5194/tc-15-4421-2021, 2021.

Dryak, M. C. and Enderlin, E. M.: Analysis of Antarctic Peninsula glacier frontal ablation rates with respect to iceberg melt-inferred variability in ocean conditions, J. Glaciol., 66, 457–470, https://doi.org/10.1017/jog.2020.21, 2020.

Fluegel, B. L. and Walker, C.: The Two-Decade Evolution of Antarctica's Hektoria Glacier and Its 2022 Rapid Retreat From Satellite Observations, Geophysical Research Letters, 51, https://doi.org/10.1029/2024GL110592, 2024.

Friedl, P., Seehaus, T. C., Wendt, A., Braun, M. H., and Höppner, K.: Recent dynamic changes on Fleming Glacier after the disintegration of Wordie Ice Shelf, Antarctic Peninsula, The Cryosphere, 12, 1347–1365, https://doi.org/10.5194/tc-12-1347-2018, 2018.

Gerrish, L., Ireland, L., Fretwell, P. T., and Cooper, P.: High resolution vector polygons of the Antarctic coastline - VERSION 7.10, 2024.

Hogg, A. E., Shepherd, A., Cornford, S. L., Briggs, K. H., Gourmelen, N., Graham, J. A., Joughin, I., Mouginot, J., Nagler, T., Payne, A. J., Rignot, E., and Wuite, J.: Increased ice flow in Western Palmer Land linked to ocean melting, Geophysical Research Letters, 44, 4159–4167, https://doi.org/10.1002/2016GL072110, 2017.

Huber, J., Cook, A. J., Paul, F., and Zemp, M.: A complete glacier inventory of the Antarctic Peninsula based on Landsat 7 images from 2000 to 2002 and other preexisting data sets, Earth Syst. Sci. Data, 9, 115–131, https://doi.org/10.5194/essd-9-115-2017, 2017.

Jekel, C. F. and Venter, G.: pwlf: A Python Library for Fitting 1D Continuous Piecewise Linear Functions, 2019.

Josey, S. A., Meijers, A. J. S., Blaker, A. T., Grist, J. P., Mecking, J., and Ayres, H. C.: Record-low Antarctic sea ice in 2023 increased ocean heat loss and storms, Nature, 636, 635–639, https://doi.org/10.1038/s41586-024-08368-y, 2024.

https://doi.org/10.5194/egusphere-2025-5492
Preprint. Discussion started: 15 December 2025

Kang, Y.-L., Kang, S.-C., Guo, W.-Q., Che, T., Jiang, Z.-L., Wang, Z.-F., Xu, Q.-Q., and Yang, C.-D.: Spatiotemporal variations in glacier area and surface velocity of the northern Antarctic Peninsula during 2018–2022, Advances in Climate Change Research, 15, 297–311, https://doi.org/10.1016/j.accre.2024.03.004, 2024.

KC, A., Enderlin, E. M., Fahrner, D., Moon, T., and Carroll, D.: Seasonality in terminus ablation rates for the glaciers in Greenland (Kalaallit Nunaat), The Cryosphere, 19, 3089–3106, https://doi.org/10.5194/tc-19-3089-2025, 2025.

Kwiatkowski, D., Phillips, P. C., Schmidt, P., and Shin, Y.: Testing the null hypothesis of stationarity against the alternative of a unit root, Journal of Econometrics, 54, 159–178, https://doi.org/10.1016/0304-4076(92)90104-Y, 1992.

Lemos, A., Shepherd, A., McMillan, M., and Hogg, A. E.: Seasonal Variations in the Flow of Land-Terminating Glaciers in Central-West Greenland Using Sentinel-1 Imagery, Remote Sensing, 10, 1878, https://doi.org/10.3390/rs10121878, 2018.

Li, T., Heidler, K., Mou, L., Ignéczi, Á., Zhu, X. X., and Bamber, J. L.: A high-resolution calving front data product for marine-terminating glaciers in Svalbard, Earth Syst. Sci. Data, 16, 919–939, https://doi.org/10.5194/essd-16-919-2024, 2024.

Loebel, E., Baumhoer, C. A., Dietz, A., Scheinert, M., and Horwath, M.: Calving front positions for 42 key glaciers of the Antarctic Peninsula Ice Sheet: a sub-seasonal record from 2013 to 2023 based on deep-learning application to Landsat multi-spectral imagery, Earth Syst. Sci. Data, 17, 65–78, https://doi.org/10.5194/essd-17-65-2025, 2025.

Moon, T., Joughin, I., and Smith, B.: Seasonal to multiyear variability of glacier surface velocity, terminus position, and sea ice/ice mélange in northwest Greenland, JGR Earth Surface, 120, 818–833, https://doi.org/10.1002/2015JF003494, 2015.

Moon, T. A., Cohen, B., Black, T. E., Laidre, K. L., Stern, H. L., and Joughin, I.: Characterizing southeast Greenland fjord surface ice and freshwater flux to support biological applications, The Cryosphere, 18, 4845–4872, https://doi.org/10.5194/tc-18-4845-2024, 2024.

Ochwat, N. E., Scambos, T. A., Banwell, A. F., Anderson, R. S., Maclennan, M. L., Picard, G., Shates, J. A., Marinsek, S., Margonari, L., Truffer, M., and Pettit, E. C.: Triggers of the 2022 Larsen B multi-year landfast sea ice breakout and initial glacier response, The Cryosphere, 18, 1709–1731, https://doi.org/10.5194/tc-18-1709-2024, 2024.

Parsons, R., Sun, S., Gudmundsson, G. H., Wuite, J., and Nagler, T.: Quantifying the buttressing contribution of landfast sea ice and melange to Crane Glacier, Antarctic Peninsula, The Cryosphere, 18, 5789–5801, https://doi.org/10.5194/tc-18-5789-2024, 2024.

Pritchard, H., Fretwell, P., Fremand, A., Bodart, J., Kirkham, J., Aitken, A., Bamber, J., Bell, R., Bianchi, C., Bingham, R., Blankenship, D., Casassa, G., Catania, G., Christianson, K., Conway, H., Corr, H., Cui, X., Damaske, D., Damn, V., Dorschel, B., Drews, R., Eagles, G., Eisen, O., Eisermann, H., Ferraccioli, F., Field, E., Forsberg, R., Franke, S., Fujita, S., Gim, Y., Goel, V., Gogineni, S. P., Greenbaum, J., Hills, B., Hindmarsh, R., Hoffman, A., Holmlund, P., Holschuh, N., Holt, J., Horlings, A., Humbert, A., Jacobel, R., Jansen, D., Jenkins, A., Jokat, W., Jordan, T., King, E., Kohler, J., Krabill, W., Langley, K., Lee, J., Leitchenkov, G., Leuschen, C., Luyendyk, B., MacGregor, J., MacKie, E., Matsuoka,

https://doi.org/10.5194/egusphere-2025-5492
Preprint. Discussion started: 15 December 2025

K., Moholdt, G., Morlighem, M., Mouginot, J., Nitsche, F., Nogi, Y., Nost, O., Paden, J., Pattyn, F., Popov, S., Kusk-Gillespie, M., Rignot, E., Rippin, D., Rivera, A., Roberts, J., Ross, N., Ruppel, A., Schroeder, D., Siegert, M., Smith, A., Steinhage, D., Studinger, M., Sun, B., Tabacco, I., Tinto, K., Urbini, S., Vaughan, D., Welch, B., Wilson, D., Young, D., and Zirizzotti, A.: BEDMAP3 - Ice thickness, bed and surface elevation for Antarctica - gridding products, 2024.

Purich, A. and Doddridge, E. W.: Record low Antarctic sea ice coverage indicates a new sea ice state, Commun Earth Environ, 4, https://doi.org/10.1038/s43247-023-00961-9, 2023.

Rack, W., Rott, H., Nagler, T., and Skvarca, P.: Areal changes and motion of northern Larsen Ice Shelf, Antarctic Peninsula, in: IGARSS '98. Sensing and Managing the Environment. 1998 IEEE International Geoscience and Remote Sensing. Symposium Proceedings. (Cat. No.98CH36174), Seattle, WA, USA, 10 July 1998 - 10 July 1998, 2243-2245 vol.4, 1998.

Rack, W. and Rott, H.: Pattern of retreat and disintegration of the Larsen B ice shelf, Antarctic Peninsula, Ann. Glaciol., 39, 505–510, https://doi.org/10.3189/172756404781814005, 2004.

Rignot, E., Casassa, G., Gogineni, P., Krabill, W., Rivera, A., and Thomas, R.: Accelerated ice discharge from the Antarctic Peninsula following the collapse of Larsen B ice shelf, Geophysical Research Letters, 31, https://doi.org/10.1029/2004GL020697, 2004.

Robel, A. A.: Thinning sea ice weakens buttressing force of iceberg mélange and promotes calving, Nature communications, 8, 14596, https://doi.org/10.1038/ncomms14596, 2017.

Rott, H., Scheiblauer, S., Wuite, J., Krieger, L., Floricioiu, D., Rizzoli, P., Libert, L., and Nagler, T.: Penetration of interferometric radar signals in Antarctic snow, The Cryosphere, 15, 4399–4419, https://doi.org/10.5194/tc-15-4399-2021, 2021.

Rott, H., Wuite, J., Rydt, J. de, Gudmundsson, G. H., Floricioiu, D., and Rack, W.: Impact of marine processes on flow dynamics of northern Antarctic Peninsula outlet glaciers, Nature communications, 11, 2969, https://doi.org/10.1038/s41467-020-16658-y, 2020.

Rott, H., Abdel Jaber, W., Wuite, J., Scheiblauer, S., Floricioiu, D., van Wessem, J. M., Nagler, T., Miranda, N., and van den Broeke, M. R.: Changing pattern of ice flow and mass balance for glaciers discharging into the Larsen A and B embayments, Antarctic Peninsula, 2011 to 2016, The Cryosphere, 12, 1273–1291, https://doi.org/10.5194/tc-12-1273-2018, 2018.

Rott, H., Rack, W., Skvarca, P., and Angelis, H. de: Northern Larsen Ice Shelf, Antarctica: further retreat after collapse, Ann. Glaciol., 34, 277–282, https://doi.org/10.3189/172756402781817716, 2002.

Rott, H., Skvarca, P., and Nagler, T.: Rapid Collapse of Northern Larsen Ice Shelf, Antarctica, Science (New York, N.Y.), 271, 788–792, https://doi.org/10.1126/science.271.5250.788, 1996.

Scambos, T., Hulbe, C., and Fahnestock, M.: Climate-Induced Ice Shelf Disintegration in the Antarctic Peninsula, in: Antarctic Peninsula Climate Variability: Historical and Paleoenvironmental Perspectives, edited by: Domack, E.,

https://doi.org/10.5194/egusphere-2025-5492
Preprint. Discussion started: 15 December 2025

Levente, A., Burnet, A., Bindschadler, R., Convey, P., and Kirby, M., American Geophysical Union, Washington, D. C., 79–92, https://doi.org/10.1029/AR079p0079, 2003.

Schmidtko, S., Heywood, K. J., Thompson, A. F., and Aoki, S.: Multidecadal warming of Antarctic waters, Science (New York, N.Y.), 346, 1227–1231, https://doi.org/10.1126/science.1256117, 2014.

Seehaus, T., Cook, A. J., Silva, A. B., and Braun, M.: Changes in glacier dynamics in the northern Antarctic Peninsula since 1985, The Cryosphere, 12, 577–594, https://doi.org/10.5194/tc-12-577-2018, 2018.

Seehaus, T., Marinsek, S., Helm, V., Skvarca, P., and Braun, M.: Changes in ice dynamics, elevation and mass discharge of Dinsmoor–Bombardier–Edgeworth glacier system, Antarctic Peninsula, Earth and Planetary Science Letters, 427, 125–135, https://doi.org/10.1016/j.epsl.2015.06.047, 2015.

Shen, Q., Wang, H., Shum, C. K., Jiang, L., Hsu, H. T., and Dong, J.: Recent high-resolution Antarctic ice velocity maps reveal increased mass loss in Wilkes Land, East Antarctica, Scientific reports, 8, 4477, https://doi.org/10.1038/s41598-018-22765-0, 2018.

Siegert, M., Atkinson, A., Banwell, A., Brandon, M., Convey, P., Davies, B., Downie, R., Edwards, T., Hubbard, B., Marshall, G., Rogelj, J., Rumble, J., Stroeve, J., and Vaughan, D.: The Antarctic Peninsula Under a 1.5°C Global Warming Scenario, Front. Environ. Sci., 7, https://doi.org/10.3389/fenvs.2019.00102, 2019.

Silva, A. B., Arigony-Neto, J., Braun, M. H., Espinoza, J. M. A., Costi, J., and Jaña, R.: Spatial and temporal analysis of changes in the glaciers of the Antarctic Peninsula, Global and Planetary Change, 184, 103079, https://doi.org/10.1016/j.gloplacha.2019.103079, 2020.

Stewart, J.: Antarctica: An Encyclopedia, 2d ed, McFarland, Incorporated, Publishers, 2011.

Strozzi, T., Luckman, A., Murray, T., Wegmuller, U., and Werner, C. L.: Glacier motion estimation using SAR offset-tracking procedures, IEEE Trans. Geosci. Remote Sensing, 40, 2384–2391, https://doi.org/10.1109/TGRS.2002.805079, 2002.

Sun, Y., Riel, B., and Minchew, B.: Disintegration and Buttressing Effect of the Landfast Sea Ice in the Larsen B Embayment, Antarctic Peninsula, Geophysical Research Letters, 50, https://doi.org/10.1029/2023GL104066, 2023.

Surawy-Stepney, T., Hogg, A. E., Cornford, S. L., Wallis, B. J., Davison, B. J., Selley, H. L., Slater, R. A. W., Lie, E. K., Jakob, L., Ridout, A., Gourmelen, N., Freer, B. I. D., Wilson, S. F., and Shepherd, A.: The effect of landfast sea ice buttressing on ice dynamic speedup in the Larsen B embayment, Antarctica, The Cryosphere, 18, 977–993, https://doi.org/10.5194/tc-18-977-2024, 2024.

Tuckett, P. A., Ely, J. C., Sole, A. J., Livingstone, S. J., Davison, B. J., van Melchior Wessem, J., and Howard, J.: Rapid accelerations of Antarctic Peninsula outlet glaciers driven by surface melt, Nature communications, 10, 4311, https://doi.org/10.1038/s41467-019-12039-2, 2019.

Ultee, L., Felikson, D., Minchew, B., Stearns, L. A., and Riel, B.: Helheim Glacier ice velocity variability responds to runoff and terminus position change at different timescales, Nature communications, 13, 6022, https://doi.org/10.1038/s41467-022-33292-y, 2022.

https://doi.org/10.5194/egusphere-2025-5492
Preprint. Discussion started: 15 December 2025

Virtanen, P., Gommers, R., Oliphant, T. E., Haberland, M., Reddy, T., Cournapeau, D., Burovski, E., Peterson, P., Weckesser, W., Bright, J., van der Walt, S. J., Brett, M., Wilson, J., Millman, K. J., Mayorov, N., Nelson, A. R. J., Jones, E., Kern, R., Larson, E., Carey, C. J., Polat, İ., Feng, Y., Moore, E. W., VanderPlas, J., Laxalde, D., Perktold, J., Cimrman, R., Henriksen, I., Quintero, E. A., Harris, C. R., Archibald, A. M., Ribeiro, A. H., Pedregosa, F., and van Mulbregt, P.: SciPy 1.0: fundamental algorithms for scientific computing in Python, Nature methods, 17, 261–272, https://doi.org/10.1038/s41592-019-0686-2, 2020.

Wallis, B. J., Hogg, A. E., Zhu, Y., and Hooper, A.: Data and code for "Change in grounding line location on the Antarctic Peninsula measured using a tidal motion offset correlation method" by Wallis et al. 2024, 2024.

Wallis, B. J., Hogg, A. E., Meredith, M. P., Close, R., Hardy, D., McMillan, M., Wuite, J., Nagler, T., and Moffat, C.: Ocean warming drives rapid dynamic activation of marine-terminating glacier on the west Antarctic Peninsula, Nature communications, 14, 7535, https://doi.org/10.1038/s41467-023-42970-4, 2023a.

Wallis, B. J., Hogg, A. E., van Wessem, J. M., Davison, B. J., and van den Broeke, M. R.: Widespread seasonal speed-up of west Antarctic Peninsula glaciers from 2014 to 2021, Nat. Geosci., 16, 231–237, https://doi.org/10.1038/s41561-023-01131-4, 2023b.

Wendt, J., Rivera, A., Wendt, A., Bown, F., Zamora, R., Casassa, G., and Bravo, C.: Recent ice-surface-elevation changes of Fleming Glacier in response to the removal of the Wordie Ice Shelf, Antarctic Peninsula, Ann. Glaciol., 51, 97–102, https://doi.org/10.3189/172756410791392727, 2010.

Werner, C., Wegmüller, U., Strozzi, T., and Wiesmann, A.: GAMMA SAR and Interferometric Processing Software, Proceedings of ERS-ENVISAT Symposium, available at: https://www.gamma-rs.ch/uploads/media/2000-1_GAMMA_Software.pdf, 2000.

York, A. V., Frey, K. E., Jamali, S., and Das, S. B.: Change Points Detected in Decadal and Seasonal Trends of Outlet Glacier Terminus Positions across West Greenland, Remote Sensing, 12, 3651, https://doi.org/10.3390/rs12213651, 2020.